

1

2 Abiotic and biotic-controlled nanomaterial formation pathways

3 within the Earth's nanomaterial cycle

4

5 Michael Schindler¹, Jie Xu² and Michael F. Hochella, Jr.³

6

7

8 ¹Department of Earth Sciences, University of Manitoba, Winnipeg, Manitoba, Canada,
9 R3T2N2, e-mail: Michael.schindler@umanitoba.ca

10 ²School of Molecular Science, Arizona State University, Tempe, Arizona, USA, 85287

11 ³Department of Geosciences, Virginia Tech, Blacksburg, Virginia, USA, 24060

12

13

14

15

16

17

18

19

20

21

22

23

24

ABSTRACT

25 Nanomaterials have unique properties and play critical roles in the budget, cycling, and
26 chemical processing of elements on Earth. An understanding of the cycling of nanomaterials
27 can be greatly improved if the pathways of their formation are clearly recognized and
28 understood. Here, we show that nanomaterial formation pathways mediated by aqueous fluids
29 can be grouped into four major categories, abiotic and biotic processes coupled and decoupled
30 from weathering processes. These can be subdivided in 18 subcategories relevant to the critical
31 zone, and environments such as ocean hydrothermal vents and the upper mantle. Similarly,
32 pathways in the gas phase such as volcanic fumaroles, wildfires and particle formation in the
33 stratosphere and troposphere can be grouped into two major groups and five subcategories. In
34 the most fundamental sense, both aqueous-fluid and gaseous pathways provide an
35 understanding of the formation of all minerals which are inherently based on nanoscale
36 precursors and reactions.

37

38 The Earth system is unimaginably complex due to the abundance and diversity of life
39 (from micro- to macro-organisms) intertwined with literally millions of organic and inorganic
40 molecules and materials composed from atoms across the periodic table. To parse the system
41 into less entangled portions, scientists have used what has become known as Earth cycles for
42 more than a century. As such, one can more easily follow important chemical aspects of the
43 planet, such as individual elements (e.g. carbon, nitrogen, or phosphorus), individual Earth
44 components (e.g. rocks, water, or nutrients), or multiple related elements/components in
45 living/non-living subsystems (e.g., one of the many useful biogeochemical cycles). Driven by the
46 expansion of available methods and tools for examining the Earth system, more Earth cycles
47 are realized and components studied, as for example Earth's nanomaterial (NM) cycle more
48 recently recognized and introduced¹. Like all cycles, the NM cycle encompasses (at least in

49 principle) where NM are, and how they form, are distributed, and then lost or consumed as a
50 next generation of nano-components appear throughout the Earth system.

51 The reason that a NM cycle is useful for Earth science, and in fact necessary in the
52 complete study of our planet, is because these materials behave differently than entities
53 generally smaller (e.g., most molecules), and bigger (e.g., most minerals, and biological
54 components such as cells, while at the same time realizing that viruses are complex organic
55 nanoparticles, and large molecules like proteins can also be considered nanoparticles). In the
56 mineral world, by far making up the bulk of this planet and a major part of the critical zone of the
57 Earth, nanominerals and mineral nanoparticles are not only abundant and widespread, but it
58 has been suggested that they have been one of the principal catalytic components of Earth
59 throughout its history¹. They may contain any element in the periodic table, may be atomically
60 ordered (crystalline), disordered, or amorphous, and range in size from less than a nanometer
61 (<0.001 microns) up to several tens of nanometers (often in the range of 0.03 to 0.05 microns).
62 Their properties depend, like bulk materials, on their chemical composition and atomic structure.
63 Changing either of these, even slightly, can result in very different chemical and/or physical
64 properties. However, for NMs, their properties also depend on their size, shape, and surface
65 topographic features. The reason that this is important is that NMs often have dramatically
66 different chemical and physical properties relative to their macro-mineral equivalent in the bulk
67 state (if one even exists with the same atomic structure), that is in sizes larger than a few to
68 several tens of nanometers in one, two, or all three dimensions. It is these property changes
69 that not only significantly impact the Earth system in many important ways, including their
70 distribution around the planet^{1, 2}, but for NMs in general, have also produced the nanoscience
71 and nanotechnology revolution in the last few decades in the medical, electronic, catalytic, and
72 chemical fields valued at trillions of US dollars worldwide each year³.

73 Formation, properties, cycling and budgets of NM's in Earth compartments (lithosphere,
74 atmosphere and hydrosphere) have been reviewed numerous times ^{4,5} with these papers also
75 focusing on specific types of NMs ^{6,7} and their role in a vast array of Earth and environmental
76 processes ⁸. However, this field is still in its infancy with new and often unexpected discoveries
77 constantly reported. In addition, research challenges are great due to chemical and physical
78 complexities of nano-processes, and the exceptionally small scales that must be navigated.

79 This review concerning the group recognition and current understanding of abiotic- and
80 biotic-controlled formation pathways is to the best of our knowledge the first of its type.
81 Pathways of NM formation can occur in highly diverse environments, for example in the
82 presence of aqueous fluids in soils, sediments, and the biological environment therein, all the
83 way to within the gases or magmas in volcanic systems. We will focus primarily on formation
84 pathways of NM mediated by aqueous fluids as those occur in the Earth's critical zone (CZ).
85 Within this zone, humans interact directly or indirectly with NMs as they impact the form and
86 function of living and non-living things. ⁹ However, we will also show that pathways of NM
87 formation similar to those observed in the CZ also occur in hydrothermal systems, as well as in
88 gas-dominated systems such as volcanic fumaroles, wildfires, and particle formation in the
89 stratosphere and lower troposphere. Addressing pathways of NM formation outside the CZ is
90 important as they also play fundamental roles, for example, in the cycling of elements, the
91 formation of ore deposits, and the radiation budget of the atmosphere.

92 Overall, we find that despite the complexity and wide-variations of abiotic and biotic-
93 controlled formation pathways mediated by aqueous fluids, they can be reasonably categorized
94 into just four general types, each embodying a few to several sub-categories. For gaseous
95 formation pathways, we have also identified two major types representing several additional
96 sub-categories. Finally, it should be stated that determining these nano-formation pathways in
97 natural environments is challenging, especially in that it requires very sophisticated transmission

98 electron microscopes with the latest analytical chemistry attachments, as well as state-of-the-art
99 sample preparation tools.

100 **Pathways of nanomaterial formation**

101 All the formation pathways described below are categorized in Tables 1-2. The great
102 majority of inorganic NM formation in the CZ consists of clay minerals due to silicate rock
103 weathering processes ¹. Clays are considered mineral nanoparticles, as they have nanoscale
104 thicknesses. This is one of the key nano-related factors that give them their unique properties.
105 However, in the weathering process, other less abundant but still critically important inorganic
106 NMs form ¹. Pathways of NM formation that are mediated by aqueous fluids also occur in the
107 deeper portions of Earth's crust at higher temperatures. These can be driven by alteration
108 processes or direct precipitation from meteoric water mixed with water from hydrothermal and/or
109 magmatic sources.

110 Abiotic and biotic-controlled formation pathways of NMs in aqueous fluids can be
111 coupled or decoupled from a weathering/alteration process (categories I versus II and III versus
112 IV; Fig. 1 and Table 1). Coupled pathways are commonly based on dissolution-precipitation
113 processes, in which the dissolution of the parent and the precipitation of the daughter(s) are
114 closely coupled in space and time (also called interface-coupled dissolution-precipitation
115 reactions ¹⁰). The key components of such a pathway are the interfacial fluid phase and the
116 porosity in the altered part of the parent phase which facilitate the mass exchange between the
117 interface (i.e. where the dissolution-precipitation occurs) and the bulk fluid. Supersaturations
118 and chemical compositions of the interfacial fluid as well as surface energies and stability of
119 potential phases control the type of daughter phases that precipitate along the interface ^{10,11}.
120 Here, we consider coupling of NM-formation and dissolution process when the formation occurs
121 in a porous alteration layer or mineral surface coating. This definition assumes that the
122 formation of the NM can be shifted in space and time and become less relevant to the

123 dissolution process. This approach also allows us to define whether biotic-controlled formations
124 of NMs are coupled or decoupled from associated weathering/alteration processes that may
125 have provided the bio-community with key nutrients and energy. The biotic-controlled NM-
126 formation is considered coupled when occurring in proximity to the “parent” dissolution sites,
127 especially within a confined space; alternatively, the formation is considered decoupled when
128 occurring far from the parent dissolution sites, independent of the mass transfer between the
129 dissolving mineral surface and the bulk solution.

130 First generation NMs may become unstable with changes in environmental conditions,
131 composition of the pore fluid, or degree of agglomeration as it undergoes weathering/alteration.
132 As a consequence, a second generation of NMs may form, and their formation may again be
133 coupled or decoupled from the dissolution of the first NM-generation (Fig. 1). An alternative
134 pathway of the first or any consecutive NM-generation is (a) their agglomeration (or flocculation)
135 and subsequent Ostwald ripening towards larger micrometer-size grains (note that Ostwald
136 ripening can be also considered a dissolution-precipitation process) or (b) their attachment on
137 the surface of a growing crystals. The latter mechanism is termed crystallization through particle
138 attachment (CPA)¹², where the attachment of the NM can occur in a random or orientated
139 fashion. For random attachment, structural re-organization is required for incorporation of the
140 NM into the bulk crystal, whereas orientated attachment requires the rotation of the NM upon
141 attachment¹³.

142

143 *A classification of abiotic-controlled pathways of nanomaterial formation in aqueous fluids (I and*
144 *II)*

145 Pathways to the NM-formation coupled with weathering/alteration processes, can be
146 further distinguished based on whether the NM is part of a first (Ia) or second or consecutive
147 NM-generation (Ib; Table 1). The formation of a first NM-generation coupled with a
148 weathering/alteration process can be then further subdivided into I. those where the parent

149 material is also a NM (*1a1*); II. the composition of the NM is controlled by the release of a minor
150 (*1a2*) or major element (*1a3*) of the parent phase; and III. multiple types of NMs form
151 simultaneously (*1a4*). Examples of pathways are listed in Table 1.

152 An example for *1a1* is the illitization of smectite to interstratified illite-smectite mixtures (I-
153 S). Following the Ostwald step rule, the pathway from smectite to I-S and to illite involves a
154 sequence of metastable phases that form via dissolution precipitation reactions ^{14,15}. This
155 pathway is favoured by temperature and has been used as an empirical geothermometer. An
156 environmental relevant pathway in this category would be the sulfurization of engineered or
157 incidental Ag nanoparticles into Ag₂S NMs ^{16,17} as the formation of the lower soluble Ag₂S
158 decreases the bioavailability of Ag in aquatic systems ¹⁸.

159 In *1a2*, the minor element in a dissolving phase will be the major constituent of the NM
160 whereas the major elements form a bulk material hosting the NM. The bulk material may also be
161 composed of nano-domains ¹⁹ that have undergone partial Ostwald ripening, but for
162 simplification purposes, are not considered NM. Pathways in this category include the alteration
163 of Cr-rich pyroxene and Au-bearing pyrite or a-arsenopyrite and the subsequent formation of
164 clinochlore and hematite/ pyrite/arsenopyrite (bulk phases) and chromite- and gold-
165 nanoparticles, respectively (Fig. 2a-b) ¹⁹⁻²¹. The subsequent weathering of clinochlore results in
166 the release of chromite nanoparticles, which appear in contrast to Cr³⁺ aqueous species less
167 susceptible to oxidation by Mn-oxide phases towards hexavalent Cr ²². The formation of gold
168 nanoparticles along the pyrite-hematite interface (Fig. 2a, b) can lead to their agglomeration and
169 formation of supergene gold deposits ²⁰.

170 Environmental relevant pathways in *1a3* include the formation of amorphous silica and
171 ferrihydrite on the surfaces of altered feldspars/plagioclase and pyrite ^{23, 24}. The formation of an
172 amorphous silica-gel coating provides nucleation sites for the subsequent formation of clay
173 minerals (see below), and the gel's reorganization (as observed for borosilicate glass) can lead
174 to the passivation of the underlying mineral ²⁵. The formation of such an armouring silica-rich

175 mineral surface coating on Ca-silicate minerals could affect the release of Ca into the ocean and
176 thus the sequestration of CO₂²⁶⁻³⁰. Similarly, the formation of ferrihydrite on pyrite and its
177 potential transformation into the more stable Fe-oxide phases goethite and hematite decreases
178 the dissolution rate of pyrite and thus the generation of acidity in mine tailings ³¹. *la3* also
179 includes the common pathway where a more soluble mineral is replaced by NMs of a less
180 soluble mineral. An example would be the replacement of Ag₂S (acanthite) by NMs composed
181 of HgS (cinnabar) (Table 1; Figure 2c-d) ³². An example for *la4* would be the simultaneous
182 formation of a silica-rich amorphous NM and ferrihydrite during the weathering of volcanic basalt
183 glass (Fig. 2e and f, ³³).

184 The formation of consecutive NM-generations (*lb*) requires the formation of a first
185 generation of NMs and is thus a subcategory of *la*. However, we treat *lb* as its own as it allows
186 for deciphering additional pathways of NM-formation. Formation of NMs of the second or
187 consecutive generation can be further subdivided into those which form from an amorphous
188 precursor (*lb1*), through the addition or removal of a minor constituent from the alteration layer
189 (*lb2*) or to the addition or removal of a major constituent to the alteration layer (*lb3*). As the NM-
190 formation in these categories often requires the addition of chemical constituents from the bulk
191 fluid, their formation is thus not entirely coupled to the weathering/alteration process of the
192 underlying mineral.

193 An example for *lb1* would be the pathways from an amorphous silica-rich precursor to
194 consecutive generations of clay minerals on the surface of an altered feldspar ³⁴ or the
195 formation of different Fe-bearing NMs from an amorphous Fe-silica-rich precursor on the
196 surface of an altered Fe-rich pyroxene (Fig. 2g and h)³⁵.

197 Pathway of *lb2* occurs, for example, during the alteration of micas. Here the pathway is
198 initiated with the hydration (addition of H₂O and OH groups) and oxidation of muscovite and
199 biotite followed by the formation of multiple generations of clay minerals on their surfaces
200 (removal of alkaline cations) ^{34,36,37}. Pathways of *lb3* include for example the formation of

201 multiple generations of Fe-hydroxides, including a first generation of nano-crystalline ferrihydrite
202 on the surface of pyrite (i.e. removal of sulfur; ^{24,38}) and the conversion of uraninite into a highly
203 disordered silica-rich uraninite (addition of silica) followed by the formation of coffinite, USiO_4
204 (this process is also called coffinization of uraninite ^{39,40}). The latter process is common in
205 uranium ore deposits and may also be relevant during the interaction of nuclear fuel waste (the
206 natural analogue to uraninite) with silica-rich fluids.

207 Formation processes decoupled from weathering processes (II) involve the transport of
208 released constituents from the dissolving mineral surface and alteration layer to areas of either
209 higher reactivity or different environmental conditions.

210 Areas of higher reactivity can be reactive surface sites on minerals or organic material
211 that chemically transform (oxidize or reduce) elements adsorbed to their surface (IIa). Reactive
212 surface sites can be also highly underbonded surface terminations along surfaces, terraces,
213 edges, or kink sites of organic matter, plants and minerals at which the initial adsorption of
214 aqueous species results in the heterogeneous nucleation of NMs (IIb). The transport of
215 constituents to areas of different environmental conditions such as pH, Eh, P, T often promote
216 the homogeneous nucleation of NMs (IIc).

217 Examples for IIa include the diffusion of Cu^{1+2+} and Ag^+ -bearing species into organic
218 matter and their reduction by organic functional groups and the subsequent formation of Cu and
219 Ag nanoparticles ^{41,42, 17,43}. A similar pathway occurs when Cu^{1+2+} -bearing species enter the
220 interlayer of Fe^{2+} -bearing phyllosilicates and become reduced by Fe^{2+} terminations along the
221 octahedra layers of the sheet silicates ⁴⁴⁻⁴⁸. Both processes are relevant to the sequestration of
222 Cu in smelter- and mining-impacted soils.

223 The heterogeneous NM-nucleation in pores or on surfaces of organic matter, minerals,
224 bacteria, fungi and plants is often induced through the provision of a nucleation site but can be
225 also controlled by the pore size and pore shape. For example, a decrease in pore diameter
226 enhances the formation of inner-sphere complexes on the surfaces of the nanopores (via a

227 decrease in the surface acidity constants of the surface functional groups) and thus leads to the
228 accumulation of NM-constituents in the pore ⁴⁹. However, a decreasing pore size also increases
229 the solubility of the material due to limiting its size (expressed in the Pore Controlled Solubility
230 (PCS) model ⁵⁰). Hence, the formation of NMs in pore spaces can be based on a combination of
231 different pathways (i.e. heterogeneous nucleation versus supersaturation) but is in this study
232 assigned to only one category. Examples for the formation of NMs in porous materials include
233 the formation of amorphous silica, Cu-(hydr)oxides and minerals of the spinel group (magnetite,
234 Fe₃O₄ and franklinite, ZnFe₂O₄) in porous organic matter in Cu-contaminated soils ⁵¹. The
235 heterogeneous nucleation of NMs was observed on reactive surfaces of fungi, plants, bacteria
236 and granite and include for example Ca-oxalate, gold, clays and schwertmannite, respectively
237 (Table 1) ⁵²⁻⁵⁵. Under hydrothermal conditions, Au and sulfide-NMs often nucleate on the
238 surfaces of pyrite or As-rich pyrite and occur within growth zones of these minerals ¹⁹.

239 Many pathways exist for the homogeneous NM-nucleation due to changes in
240 environmental conditions ^{34,56,57} (IIc). One important pathway affecting the transport of the
241 nutrient Fe to the ocean is the formation of ferrihydrite in riverine or riparian zones due to
242 changes in pH and Eh, respectively ^{58,59}.

243 An important ore forming process is the pathway from dissolved metals in hydrothermal
244 fluids to sulfate, sulfide and native element NMs around black smokers ^{60,61} and in hydrothermal
245 veins ⁶². The pathway of their formation is initiated by the boiling of the hydrothermal fluids due
246 to a decrease in pressure, the mixing of the fluids, and the loss of reducing gases such as H₂S
247 and H₂ which subsequently result in the oxidation of redox-sensitive ions, an increase in the
248 respective saturation indices, and homogeneous NM-nucleation.

249

250 *A classification of biotic-controlled pathways of NM formation in aqueous fluids*

251 The presence of naturally occurring NMs may play important, if not essential, roles in
252 enabling and sustaining microbial metabolisms. Living organisms may be involved in the NM

253 formation through three ways: (1) directly utilizing a substrate (as an energy or nutrient source)
254 and transform it into NMs (categories IIIa and IVa, Table 1); (2) actively control NM formation
255 using their biomolecular toolbox (IIIb and IVb, Table 1); and (3) passively cause NM formation
256 through discharging metabolites into their immediate surroundings and through the presence of
257 their cell surfaces and extracellular polymeric substances (EPS) (IIIc, IIId, and IVc, Table 1).

258 Most biotic NM-formations are considered decoupled (IVa, b, and c, Table 1) unless the
259 substrate fueling the biological growth and subsequent NM formation is trackable or physically
260 restricted within the biological communities responsible for the NM formation (IIIa, b, c, and d,
261 Table 1). The coupled scenarios include bio-utilization of solid-phase substrate (IIIa and b, Fig
262 3) and NM formation within a confined space mediated by biological metabolisms, e.g., biofilms
263 in the proximity to where the substrate is mobilized (IIIc, Fig 3). It is noted that the biotic NMs in
264 IIIa versus IIIb (Fig. 3), despite their mineralogical similarities, may reflect distinctive formation
265 processes based on their morphologies and size distributions. The former (IIIa) was likely a
266 result of microbial reduction of pre-existing Fe(III) phases⁶³ whereas the latter likely involved
267 actively controlled intracellular biomineralization⁶⁴.

268 The biotic NMs formed through active biomineralization more likely behave as functional
269 and flexible “nano tools” that may assist the biological cells or community with electron transfer,
270 chemotaxis, and substrate storage⁶⁵. In these cases (IIIb and IVb, Table 1), the cells precisely
271 control of the NM’s size, crystal structure, and stability through involving proteins, nucleic acids,
272 and other biomolecules. For example, magnetite/greigite inclusions in magnetotactic bacteria as
273 nano-compasses⁶⁶, elemental sulphur inclusions in sulfur-oxidizing microbes as nano-
274 stockpiles⁶⁷ (although the sulfur NM formation is also a result of direct energy metabolism), and
275 nano-carbonate inclusions in cyanobacteria that likely regulate the cells buoyancy⁶⁸ (Fig. 3h-i),
276 all belong to the active biotic NM-formation category. Except for the cases where organisms use
277 pre-existing phases restricted in their mass transfer within a confined space (e.g., Fig. 3b-c),
278 most functional biogenic NMs are considered decoupled (IVb).

279 In comparison to active biotic NM-formation, it is more common to find their passive
280 counterparts in nature. Passive biotic NM formation occurs simply due to the adsorption,
281 reduction, and concentrating effects of the cell surfaces and EPS matrices, or due to metabolite
282 (i.e., carbonate, sulfide, and ferric iron species etc.) accumulation in the biological
283 microenvironments. In these cases, purposely biomolecular control of the NM-formation has not
284 been identified (IIlc, IVc, and IIId). The passive formations that involve nucleation/condensation
285 from dissolved species are considered decoupled processes in terms of NM-evolution, and
286 those in which the mobility of precursor phases is restricted (e.g., in biofilms, Fig. 3d-e)^{69,70} are
287 considered coupled processes. If the NM-formation involves toxic heavy metals, these
288 processes may help to detoxify the living organisms' immediate surrounding environment (Fig.
289 3j). Biological EPS matrices may facilitate new exopolymer NM formation out of the pre-existing
290 polymeric components (IIId, Table 1)⁷¹. They may also concentrate mobile metal species
291 through chelation and biosorption^{72,73}, which occasionally lead to NM formation^{74,75}. We note
292 that the category IVc in Table 1 is inclusive of decoupled, EPS-mediated NM formation
293 processes as naturally occurring microbial communities, by default, exist as biofilms with EPS
294 matrices. Although EPS of biological flocculates have been previously reported as effective
295 traps and stabilizers for pre-existing, mostly engineered nanoparticles in the environment, the
296 focus of this paper is on the formation pathways of naturally occurring NMs, and thus we will not
297 elaborate on this aspect.

298

299 *A classification of abiotic-controlled pathways of nanomaterial formation in gases (V)*

300 The majority of particles formed in gases occur in the atmosphere. Their sizes ranges
301 from 1 nm to 100 μm with coarser particles originating from sea spray and volcanic activities
302 and finer particles from combustion and particle formation via gas-to-particle conversions⁷⁶. All
303 these processes result in the formation of NMs, which often occur in a higher number than their
304 micrometer-size counterparts.

305 Similar to pathways mediated by aqueous fluids, the formation of NM in gases can
306 include alteration of a first generation of NM or bulk materials as well as the heterogeneous and
307 homogeneous nucleation ^{77,78}. Because the role of surfaces for the formation of NM from gases
308 is less explored in the geoscience literature relative to those in soils, sediments and aqueous
309 fluids, we group the pathways of NM formation in gases on the basis of their ambient
310 temperature (Va and Vb Table 2).

311 High-T pathways of NM formation in gases occur during incidental combustion of plants
312 (wildfires) ⁷⁹ and coal (coal combustion) ⁸⁰ (Va1, Table 2), and also during volcanic eruptions
313 and within and in the vicinity of volcanic fumaroles (Va2). The pathways of NM formation during
314 wildfires and coal combustion are complex and generally not well understood. They are strongly
315 temperature dependent and occur via the thermal decomposition and volatilization of the C-
316 based material, the release of metals and volatile elements such as H, N, O, S, Cl and Se, and
317 the alteration of soil/sediment constituents. For example, NM composed of soot, nanotubes,
318 fullerenes and tar form during (or shortly after) the combustion process, S-, N-, Cl- and Se-
319 bearing phases during sublimation and solidification of hot gasses and liquids, and oxides
320 during thermal alteration of hydroxides, clay minerals and carbonates (Table 2) ⁸¹⁻⁸³.

321 Pathways of NM in gases during volcanic activities (Va2) include processes during
322 eruptions and fumarolic activities. During eruptions, silica can be reduced by carbon monoxide
323 to SiO and subsequently oxidized resulting in the nucleation of cristobalite NM ⁸⁴. Volcanic
324 fumaroles are known to deposit minerals on surfaces of rocks and sediments such as native
325 sulfur. Among these phases, nanoparticles of gold were identified at numerous locations ^{85,86}.

326 Low-T NM pathways in gases (Vb) occur in stratosphere, troposphere and critical zone
327 environments. In the troposphere and stratosphere, the freezing of water-containing HNO_3 and
328 H_2SO_4 leads to the formation of ice and crystalline acid hydrates such as $\text{H}_2\text{SO}_4 \cdot 4\text{H}_2\text{O}$ and
329 $\text{HNO}_3 \cdot 3\text{H}_2\text{O}$, an important process during annual polar ozone depletion ⁷⁵. In the troposphere,
330 emitted volatile gases from the biosphere, volcanic activities and anthroposphere such as SO_2 ,

331 NH₃, or volatile organic compounds are oxidized to low volatile trace vapors through
332 atmospheric oxidation, a process commonly referred to as new particle formation ⁸⁷. This
333 process leads first to the formation of molecular clusters and subsequently to the nucleation and
334 growth of larger aerosols ⁸⁸, which are defined as liquid or solid particles suspended in a gas
335 phase. Aerosol particles influence global climate change ⁸⁹ and impact human health ⁹⁰. In the
336 upper CZ and lower troposphere, the formation of salt NM from sea spray occurs through
337 heterogeneous and homogeneous nucleation from a fluid-gas mixture and results predominantly
338 in the formation of halite (NaCl), gypsum (CaSO₄(H₂O)₂) and other sulfates (Table 2) ⁷⁷.

339 The formation of NMs in the gas phase often has an impact on human health. For
340 example, the TiO₂ phases rutile, anatase and brookite transform into toxic O-deficient Ti_xO_{2x-1}
341 Magnéli phases during coal combustion. The phases occur as NMs (tens to hundreds of nm in
342 diameter) and are significant air pollutants in regions where coal fire plants contribute to PM
343 ^{91,92}. Furthermore, the formation of NMs during the recent high frequencies and sizes of wildfires
344 (e.g. 3.8 million hectares burned in the western USA in 2020) resulted in airborne NMs (as a
345 part of fine particulate matter, diameter $\leq 2.5 \mu\text{m}$; PM_{2.5}) which (a) have the ability to penetrate
346 deep into lungs ⁹³, (b) can contain harmful metals from anthropogenic sources (construction and
347 automotive) ⁹⁴ and (c) can mix with other atmospheric pollutants and NM formed during low T
348 pathways ⁷⁷. Health studies have shown that wildfire PM_{2.5} is more harmful than PM_{2.5} emitted
349 from many urban environments ⁹⁵.

350

351 *A classification of abiotic-controlled pathways of nanomaterial formation in magmas (VI)*

352 Pathways of NM formation during magmatic processes are commonly controlled through
353 changes in temperature, O₂-fugacity, silica- or sulfide-activity. An economically important
354 process is the formation of platinum group element (PGE) NMs in mafic or ultramafic sulfide- or
355 silicate-melts ⁷⁸ (Table 2). The pathway of their formation resembles those of category Ib, where
356 minor elements in a mineral form NMs upon weathering/alteration of their original host. Field

357 observations and experimental studies suggest that the highly siderophile and chalcophile
358 PGEs segregate from mafic or ultramafic magmas initially into metal-rich immiscible melts
359 (containing O, S, As, Te and Bi), followed by the formation of clusters and PGE-bearing NMs.
360 The PGE-bearing NMs are commonly associated with ultra-mafic minerals such as chromite,
361 pentlandite, chalcopyrite and pyrrhotite ⁹⁶⁻⁹⁸.

362

363 *Overall assessment of Earth NM formation pathways*

364 This assessment shows that the formation of nanomaterials mediated by aqueous fluids
365 within the critical zone, as well as in many other Earth environments, follow four principal
366 pathways which can be further subdivided into 10 abiotic and 6 biotic pathways (Table 1).
367 Among these pathways, the most common are very likely those occurring in soils and regoliths
368 (keeping in mind that nanomaterial formation in the oceans has not been thoroughly explored).
369 From an economic viewpoint however, the role of NMs in the formation of ore deposits is
370 especially intriguing as these nanoparticles provide an explanation for the transport of elements
371 of low solubility such as Au in hydrothermal solutions ⁹⁹. In this regard, Au NM can form via five
372 different pathways, ranging from abiotic and biotic pathways in an aqueous fluid to depositions
373 during volcanic fumarole activity (Tables 1 and 2). This high number of pathways is most likely
374 due to Au's low solubility and low compatibility with the structure of pyrite (i.e. which depends on
375 T and the amount of As in the mineral).

376 Also, of great interest is the fact that the classification of inorganic- and organic-based
377 pathways for NM formation based on factors such as multiple generations, amorphous
378 precursors, energy resources, and heterogeneous and homogeneous nucleation now allow for
379 comparisons of NM formations pathways that occur in very different chemical and physical
380 environments. These include comparisons between NM formations during the weathering of
381 silicates versus sulfides or between those in soils versus hydrothermal solutions. Hence, this
382 formation pathway compilation allows for future studies by other researchers to identify

383 formation pathways of NM similar to those observed in this study, even though the formation
384 environment is not necessarily in geologic environments discussed in this paper. An example of
385 this is the recent observation that the alteration of Cd-bearing sphalerite (ZnS) leads to the
386 formation of greenockite (CdS) NMs¹⁰⁰. This example follows the same pathway as the
387 formation of gold NMs during the alteration of Au-bearing pyrite^{19,20}, chromite NMs during the
388 alteration of Cr-rich pyroxenes²¹, rutile NMs formed during the alteration of Ti-bearing quartz,
389 and platinum group element (PGE) NMs formed during the alteration of PGE-bearing chromite
390⁷⁸.

391 Finally, as mentioned above, the discovery and delineation of all of the
392 chemical/physical/biological-based pathways of NM formation in both aqueous and gaseous
393 mediated systems will result in a better understanding of the NM cycle of the Earth as a fully
394 connected and evolving system¹. There is also the possibility (likelihood) that completely new
395 and/or novel NM formation pathways will be discovered. Such conceptual frameworks have
396 been shown repeatedly to have great value, e.g. the rock cycle, the water cycle, and the many
397 chemical cycles of the Earth. Ultimately, the nano-reactants that appear through this cycle,
398 including those NMs that only exist for very short times, consequently impact the entire Earth
399 system (atmosphere, hydrosphere, and terrestrial Earth) in highly consequential ways as has
400 been recently reviewed¹.

401

402 **Methods**

403 Features of nanomaterials published in previous studies are shown in this review. These TEM
404 images and STEM-EDS chemical distribution maps were processed with the TEM Imaging &
405 Analysis (a trademark of FEI) and Esprit 1 (a trademark of Bruker Nano) software.

406

407

408

409 **Data availability**

410 Data sharing is not applicable to this article as no datasets were generated or analysed during
411 the current study.

412

413 **Acknowledgements**

414  acknowledge financial support from a NSERC Discovery grant (RGPIN-2023-04726) to M.S.
415 M.H. acknowledges support from Virginia Tech's NanoEarth (NSF Award 2025151) and the
416 Office of Faculty Affairs.

417 We thank three anonymous reviewers for their thorough and constructive comments and
418 suggestions.

419

420 **Author contributions**

421 All authors jointly wrote the paper. MS had the idea for the review, conducted data analysis for
422 the abiotic pathways and wrote the abiotic section. JX compiled the data for the biotic pathways
423 and wrote the biotic section. MH wrote the introduction, and the last section entitled "Overall
424 assessment of Earth NM formation pathways".

425

426 **Competing interests**

427 The authors declare no competing interests.

428

429 **References**

430

431 1 Hochella, M. F., Jr. *et al.* Natural, incidental, and engineered nanomaterials and their impacts on
432 the Earth system. *Science* **363**, doi:10.1126/science.aaau8299 (2019).

433 2 Hochella, M., Aruguete, D., Kim, B. & Elwood Madden, A. in *Naturally occurring inorganic
434 nanoparticles: General assessment and a global budget for one of earth's last unexplored major
435 geochemical components* (ed In: Nature's Nanostructures) 1-42 ((A.S. Barnard, H. Guo, Eds.)
436 Pan Stanford Publishing, Singapore., 2012).

437 3 Malik, S., Muhammad, K. & Waheed, Y. Nanotechnology: A Revolution in Modern Industry.
438 *Molecules* **28**, doi:10.3390/molecules28020661 (2023).

439 4 Banfield, J. F. & Zhang, H. Nanoparticles in the Environment. *Reviews in Mineralogy and*
440 *Geochemistry* **44**, 1-58, doi:10.2138/rmg.2001.44.01 (2001).

441 5 Ju, Y. *et al.* Nanoparticles in the Earth surface systems and their effects on the environment and
442 resource. *Gondwana Research* **110**, 370-392, doi:<https://doi.org/10.1016/j.gr.2022.02.012>
443 (2022).

444 6 Guo, H. & Barnard, A. S. Naturally occurring iron oxide nanoparticles: morphology, surface
445 chemistry and environmental stability. *Journal of Materials Chemistry A* **1**, 27-42,
446 doi:10.1039/C2TA00523A (2013).

447 7 Wilson, M. J. The origin and formation of clay minerals in soils: past, present and future
448 perspectives. *Clay Minerals* **34**, 7-25, doi:10.1180/000985599545957 (1999).

449 8 Waychunas, G. A., Kim, C. S. & Banfield, J. F. Nanoparticulate Iron Oxide Minerals in Soils and
450 Sediments: Unique Properties and Contaminant Scavenging Mechanisms. *Journal of*
451 *Nanoparticle Research* **7**, 409-433, doi:10.1007/s11051-005-6931-x (2005).

452 9 Hochella, M. F. *et al.* Nanominerals, Mineral Nanoparticles, and Earth Systems. *Science* **319**,
453 1631-1635, doi:doi:10.1126/science.1141134 (2008).

454 10 Putnis, A. Mineral Replacement Reactions. *Reviews in Mineralogy and Geochemistry* **70**, 87-124,
455 doi:10.2138/rmg.2009.70.3 (2009).

456 11 Navrotsky, A., Ma, C., Lilova, K. & Birkner, N. Nanophase Transition Metal Oxides Show Large
457 Thermodynamically Driven Shifts in Oxidation-Reduction Equilibria. *Science* **330**, 199-201,
458 doi:doi:10.1126/science.1195875 (2010).

459 12 De Yoreo, J. J. *et al.* CRYSTAL GROWTH. Crystallization by particle attachment in synthetic,
460 biogenic, and geologic environments. *Science* **349**, aaa6760, doi:10.1126/science.aaa6760
461 (2015).

462 13 Zhang, H., De Yoreo, J. J. & Banfield, J. F. A Unified Description of Attachment-Based Crystal
463 Growth. *ACS Nano* **8**, 6526-6530, doi:10.1021/nn503145w (2014).

464 14 Bauluz, B., Peacor, D. R. & Ylagan, R. F. Transmission electron microscopy study of smectite
465 illitization during hydrothermal alteration of a rhyolitic hyaloclastite from Ponza, Italy. *Clays and*
466 *Clay Minerals* **50**, 157-173, doi:10.1346/000986002760832766 (2002).

467 15 Srodon, J. Nature of Mixed-Layer Clays and Mechanisms of their Formation and Alteration.
468 *Annual Review of Earth and Planetary Sciences* **27**, 19-53, doi:10.1146/annurev.earth.27.1.19
469 (2003).

470 16 Zuykov, M. *et al.* Periostracum of bivalve mollusk shells for sampling engineered metal
471 nanoparticles: A case study of silver-based nanoparticles in Canada's experimental lake.
472 *Chemosphere* **303**, 134912, doi:10.1016/j.chemosphere.2022.134912 (2022).

473 17 Akbari Alavijeh, M. *et al.* Nanoscale characterization of the sequestration and transformation of
474 silver and arsenic in soil organic matter using atom probe tomography and transmission electron
475 microscopy. *Environmental Science: Processes & Impacts* **25**, 577-593, doi:10.1039/D2EM00332E
476 (2023).

477 18 Lowry, G. V., Gregory, K. B., Apte, S. C. & Lead, J. R. Transformations of Nanomaterials in the
478 Environment. *Environmental Science & Technology* **46**, 6893-6899, doi:10.1021/es300839e
479 (2012).

480 19 Palenik, C. S. *et al.* "Invisible," gold revealed: Direct imaging of gold nanoparticles in a Carlin-type
481 deposit. *American Mineralogist* **89**, 1359-1366, doi:doi:10.2138/am-2004-1002 (2004).

482 20 Hastie, E. C. G., Schindler, M., Kontak, D. J. & Lafrance, B. Transport and coarsening of gold
483 nanoparticles in an orogenic deposit by dissolution–reprecipitation and Ostwald ripening.
484 *Communications Earth & Environment* **2**, 57, doi:10.1038/s43247-021-00126-6 (2021).

485 21 Schindler, M., Berti, D. & Hochella, M. Previously unknown mineral-nanomineral relationships
486 with important environmental consequences: The case of chromium release from dissolving
487 silicate minerals. *American Mineralogist* **102**, 2142-2145, doi:10.2138/am-2017-6170 (2017).

488 22 McClenaghan, N. W. & Schindler, M. Release of chromite nanoparticles and their alteration in
489 the presence of Mn-oxides. *American Mineralogist* **107**, 642-653, doi:10.2138/am-2021-7881
490 (2022).

491 23 Romero, R., Robert, M., Elsass, F. & Garcia, C. Evidence by transmission electron microscopy of
492 weathering microsystems in soils developed from crystalline rocks. *Clay Minerals* **27**, 21-33,
493 doi:10.1180/claymin.1992.027.1.03 (1992).

494 24 Gu, X., Heaney, P. J., Reis, F. & Brantley, S. L. Deep abiotic weathering of pyrite. *Science* **370**,
495 doi:10.1126/science.abb8092 (2020).

496 25 Gin, S. *et al.* Dynamics of self-reorganization explains passivation of silicate glasses. *Nature
497 Communications* **9**, 2169, doi:10.1038/s41467-018-04511-2 (2018).

498 26 Berner, R. A. & Maasch, K. A. Chemical weathering and controls on atmospheric O₂ and CO₂:
499 Fundamental principles were enunciated by J. J. Ebelmen in 1845. *Geochimica et Cosmochimica
500 Acta* **60** (1996).

501 27 Dixon, J. L. & von Blanckenburg, F. Soils as pacemakers and limiters of global silicate weathering.
502 *Comptes Rendus Geoscience* **344**, 597-609, doi:<https://doi.org/10.1016/j.crte.2012.10.012>
503 (2012).

504 28 Eiriksdottir, E. S., Gislason, S. R. & Oelkers, E. H. Direct evidence of the feedback between
505 climate and nutrient, major, and trace element transport to the oceans. *Geochimica et
506 Cosmochimica Acta* **166**, 249-266, doi:10.1016/j.gca.2015.06.005 (2015).

507 29 Frings, P. J. & Buss, H. L. The Central Role of Weathering in the Geosciences. *Elements* **15**, 229-
508 234, doi:10.2138/gselements.15.4.229 (2019).

509 30 Hellmann, R. *et al.* Unifying natural and laboratory chemical weathering with interfacial
510 dissolution-reprecipitation: A study based on the nanometer-scale chemistry of fluid-silicate
511 interfaces. *Chemical Geology* **294-295**, 203-216,
512 doi:<https://doi.org/10.1016/j.chemgeo.2011.12.002> (2012).

513 31 Huminicki, D. M. C. & Rimstidt, J. D. Iron oxyhydroxide coating of pyrite for acid mine drainage
514 control. *Applied Geochemistry* **24**, 1626-1634,
515 doi:<https://doi.org/10.1016/j.apgeochem.2009.04.032> (2009).

516 32 Schindler, M., Loria, A., Ramos-Arroyoc, Y. R. & Wang, F. Nano-mineral assemblages in mercury-
517 and silver-contaminated soils: records of sequestration, transformation, and release of mercury-
518 and silver-bearing nanoparticles. *Environmental Sciences: Processes and Impacts* **26**, 483-498,
519 doi:<https://doi.org/10.1039/D3EM00302G> (2023).

520 33 Schindler, M., Michel, S., Batchelder, D. & Hochella, M. F. A nanoscale study of the formation of
521 Fe-(hydr)oxides in a volcanic regolith: Implications for the understanding of soil forming
522 processes on Earth and Mars. *Geochimica et Cosmochimica Acta* **264**, 43-66,
523 doi:<https://doi.org/10.1016/j.gca.2019.08.008> (2019).

524 34 Banfield, J. F. & Eggleton, R. A. Analytical Transmission Electron Microscope Studies of
525 Plagioclase, Muscovite, and K-Feldspar Weathering. *Clays and Clay Minerals* **38**, 77-89,
526 doi:10.1346/CCMN.1990.0380111 (1990).

527 35 Schindler, M. & Hochella, M. F., Jr. Soil memory in mineral surface coatings: Environmental
528 processes recorded at the nanoscale. *Geology* **43**, 415-418, doi:10.1130/G36577.1 (2015).

529 36 Dong, H., Peacor, D. R. & Murphy, S. F. TEM study of progressive alteration of igneous biotite to
530 kaolinite throughout a weathered soil profile. *Geochimica et Cosmochimica Acta* **62**, 1881-1887,
531 doi:10.1016/s0016-7037(98)00096-9 (1998).

532 37 Jeong, G. & Kim, H. Mineralogy, chemistry, and formation of oxidized biotite in the weathering
533 profile of granitic rocks. *American Mineralogist* **88**, 352-364, doi:10.2138/am-2003-2-312 (2003).

534 38 Petrunic, B. M., Al, T. A., Weaver, L. & Hall, D. Identification and characterization of secondary
535 minerals formed in tungsten mine tailings using transmission electron microscopy. *Applied
536 Geochemistry* **24**, 2222-2233, doi:<https://doi.org/10.1016/j.apgeochem.2009.09.014> (2009).

537 39 Fayek, M., Utsunomiya, S., Ewing, R. C., Riciputi, L. R. & Jensen, K. A. Oxygen isotopic
538 composition of nano-scale uraninite at the Oklo-Okélobondo natural fission reactors, Gabon.
539 **88**, 1583-1590, doi:doi:10.2138/am-2003-1021 (2003).

540 40 Evins, L. Z. & Jensen, K. *Review of spatial relations between uraninite and coffinite - Implications
541 for alteration mechanisms*. Vol. 1475 (2011).

542 41 Lovering, T. S. Organic precipitation of metallic copper: Chapter C in Contributions to economic
543 geology (short papers and preliminary reports), 1927: Part I - Metals and nonmetals except
544 fuels. Report No. 795C, 45-52 (Washington, D.C., 1927).

545 42 Fulda, B., Voegelin, A., Ehlert, K. & Kretzschmar, R. Redox transformation, solid phase speciation
546 and solution dynamics of copper during soil reduction and reoxidation as affected by sulfate
547 availability. *Geochimica et Cosmochimica Acta* **123**, 385-402, doi:10.1016/j.gca.2013.07.017
548 (2013).

549 43 Mantha, H., Schindler, M. & Hochella, M. F. Occurrence and formation of incidental metallic Cu
550 and CuS nanoparticles in organic-rich contaminated surface soils in Timmins, Ontario.
551 *Environmental Science: Nano* **6**, 163-179, doi:10.1039/C8EN00994E (2019).

552 44 Ilton, E. S. & Veblen, D. R. Copper inclusions in sheet silicates from porphyry Cu deposits. *Nature*
553 **334**, 516-518, doi:10.1038/334516a0 (1988).

554 45 Ilton, E. S. & Veblen, D. R. Origin and mode of copper enrichment in biotite from rocks
555 associated with porphyry copper deposits; a transmission electron microscopy investigation.
556 *Economic Geology* **88**, 885-900 (1993).

557 46 IltonEugene, S., EarleyDrummondli.l, MarozasDianne, C. & VeblenDavid, R. Reaction of some
558 trioctahedral micas with copper sulfate solutions at 25 degrees C and 1 atmosphere; an electron
559 microscope and TEM investigation. *Economic Geology and the Bulletin of the Society of
560 Economic Geologists* **87**, 1813-1829, doi:10.2113/gsecongeo.87.7.1813 (1992).

561 47 Markl, G. & Bucher, K. Reduction of Cu (super 2+) in mine waters by hydrolysis of ferrous sheet
562 silicates. *European Journal of Mineralogy* **9**, 1227-1235 (1997).

563 48 Suárez, S., Nieto, F., Velasco, F. & Martín, F. J. Serpentine and chlorite as effective Ni-Cu sinks
564 during weathering of the Aguablanca sulphide deposit (SW Spain). TEM evidence for metal-
565 retention mechanisms in sheet silicates. *European Journal of Mineralogy* **23**, 179-196,
566 doi:10.1127/0935-1221/2011/0023-2084 (2011).

567 49 Wang, Y., Bryan, C., Xu, H. & Gao, H. Nanogeochimistry: Geochemical reactions and mass
568 transfers in nanopores. *Geology* **31**, 387-390, doi:10.1130/0091-
569 7613(2003)031<0387:NGRAMT>2.0.CO;2 (2003).

570 50 Stack, A. G. Precipitation in Pores: A Geochemical Frontier. *Reviews in Mineralogy and
571 Geochemistry* **80**, 165-190, doi:10.2138/rmg.2015.80.05 (2015).

572 51 Jadoon, S. *et al.* Atom probe tomography and transmission electron microscopy: a powerful
573 combination to characterize the speciation and distribution of Cu in organic matter.
574 *Environmental Science: Processes & Impacts* **24**, 1228-1242, doi:10.1039/D2EM00118G (2022).

575 52 Wallander, H., Johansson, L. & Pallon, J. PIXE analysis to estimate the elemental composition of
576 ectomycorrhizal rhizomorphs grown in contact with different minerals in forest soil. *FEMS
577 Microbiology Ecology* **39**, 147-156, doi:[https://doi.org/10.1016/S0168-6496\(01\)00209-4](https://doi.org/10.1016/S0168-6496(01)00209-4) (2002).

578 53 Douglas, S. & Beveridge, T. J. Mineral formation by bacteria in natural microbial communities.
579 *FEMS Microbiology Ecology* **26**, 79-88, doi:10.1111/j.1574-6941.1998.tb00494.x (1998).

580 54 Durocher, J. L. & Schindler, M. Iron-hydroxide, iron-sulfate and hydrous-silica coatings in acid-
581 mine tailings facilities: A comparative study of their trace-element composition. *Applied
582 Geochemistry* **26**, 1337-1352, doi:<https://doi.org/10.1016/j.apgeochem.2011.05.007> (2011).

583 55 Keshavarzi, M., Davoodi, D., Pourseyedi, S. & Taghizadeh, S. The effects of three types of alfalfa
584 plants (*Medicago sativa*) on the biosynthesis of gold nanoparticles: an insight into phytomining.
585 *Gold Bulletin* **51**, doi:10.1007/s13404-018-0237-0 (2018).

586 56 Thanh, N. T. K., Maclean, N. & Mahiddine, S. Mechanisms of Nucleation and Growth of
587 Nanoparticles in Solution. *Chemical Reviews* **114**, 7610-7630, doi:10.1021/cr400544s (2014).

588 57 Polte, J. Fundamental growth principles of colloidal metal nanoparticles – a new perspective.
589 *CrystEngComm* **17**, 6809-6830, doi:10.1039/C5CE01014D (2015).

590 58 Neubauer, E., Köhler, S. J., von der Kammer, F., Laudon, H. & Hofmann, T. Effect of pH and
591 stream order on iron and arsenic speciation in boreal catchments. *Environ Sci Technol* **47**, 7120-
592 7128, doi:10.1021/es401193j (2013).

593 59 Vasyukova, E. V. *et al.* Trace elements in organic- and iron-rich surficial fluids of the boreal zone:
594 Assessing colloidal forms via dialysis and ultrafiltration. *Geochimica et Cosmochimica Acta* **74**,
595 449-468, doi:10.1016/j.gca.2009.10.026 (2010).

596 60 Gartman, A. *et al.* Boiling-induced formation of colloidal gold in black smoker hydrothermal
597 fluids. *Geology* **46**, doi:10.1130/G39492.1 (2017).

598 61 Gartman, A. *et al.* The role of nanoparticles in mediating element deposition and transport at
599 hydrothermal vents. *Geochimica et Cosmochimica Acta* **261**, doi:10.1016/j.gca.2019.06.045
600 (2019).

601 62 Saunders, J. A. Colloidal transport of gold and silica in epithermal precious-metal systems:
602 Evidence from the Sleeper deposit, Nevada. *Geology* **18**, 757-760, doi:10.1130/0091-
603 7613(1990)018<0757:CTOGAS>2.3.CO;2 (1990).

604 63 Channell, J. E. T. *et al.* Biogenic magnetite, detrital hematite, and relative paleointensity in
605 Quaternary sediments from the Southwest Iberian Margin. *Earth and Planetary Science Letters*
606 **376**, 99-109, doi:<https://doi.org/10.1016/j.epsl.2013.06.026> (2013).

607 64 Robie, R. A. & Bethke, P. M. Molar volumes and densities of minerals. Report No. 822, 39 (1962).

608 65 Mansor, M. & Xu, J. Benefits at the nanoscale: a review of nanoparticle-enabled processes
609 favouring microbial growth and functionality. *Environmental Microbiology* **22**, 3633-3649,
610 doi:<https://doi.org/10.1111/1462-2920.15174> (2020).

611 66 Posfai, M., Buseck, P. R., Bazylinski, D. A. & Frankel, R. B. Iron sulfides from magnetotactic
612 bacteria; structure, composition, and phase transitions. *American Mineralogist* **83**, 1469-1481,
613 doi:10.2138/am-1998-11-1235 (1998).

614 67 Findlay, A. J. Microbial impact on polysulfide dynamics in the environment. *FEMS Microbiol Lett*
615 **363**, doi:10.1093/femsle/fnw103 (2016).

616 68 Benzerara, K. *et al.* Intracellular Ca-carbonate biomineralization is widespread in cyanobacteria.
617 *Proceedings of the National Academy of Sciences of the United States of America* **111**, 10933-
618 10938, doi:10.1073/pnas.1403510111 (2014).

619 69 Fairbrother, L. *et al.* Supergene gold transformation: Biogenic secondary and nano-particulate
620 gold from arid Australia. *Chemical Geology* **320-321**, 17-31,
621 doi:<https://doi.org/10.1016/j.chemgeo.2012.05.025> (2012).

622 70 Reith, F. *et al.* Biological role in the transformation of platinum-group mineral grains. *Nature
623 Geoscience* **9**, 294-298, doi:10.1038/ngeo2679 (2016).

624 71 Shammi, M., Pan, X., Mostofa, K. M. G., Zhang, D. & Liu, C.-Q. Photo-flocculation of microbial
625 mat extracellular polymeric substances and their transformation into transparent exopolymer
626 particles: Chemical and spectroscopic evidences. *Scientific Reports* **7**, 9074, doi:10.1038/s41598-
627 017-09066-8 (2017).

628 72 Costa, O. Y. A., Raaijmakers, J. M. & Kuramae, E. E. Microbial Extracellular Polymeric Substances:
629 Ecological Function and Impact on Soil Aggregation. *Frontiers in Microbiology* **9** (2018).

630 73 Flemming, H.-C. & Wingender, J. The biofilm matrix. *Nature Reviews Microbiology* **8**, 623-633,
631 doi:10.1038/nrmicro2415 (2010).

632 74 Koenigsmark, F. *et al.* Crystal lattice defects in nanocrystalline metacinnabar in contaminated
633 streambank soils suggest a role for biogenic sulfides in the formation of mercury sulfide phases.
634 *Environmental Science: Processes & Impacts* **25**, 445-460, doi:10.1039/D1EM00549A (2023).

635 75 Martin, S. T. Phase Transitions of Aqueous Atmospheric Particles. *Chem Rev* **100**, 3403-3454,
636 doi:10.1021/cr990034t (2000).

637 76 Anastasio, C. & Martin, S. T.

638 77 Donado, E. B. *et al.* Insights into the mixing of particulate matter and aerosols from different
639 sources in a Caribbean industrial town: composition and possible health effect. *Air Quality,
640 Atmosphere & Health* **16**, 1291-1310, doi:10.1007/s11869-023-01342-z (2023).

641 78 González-Jiménez, J. M. & Reich, M. An overview of the platinum-group element nanoparticles
642 in mantle-hosted chromite deposits. *Ore Geology Reviews* **81**, 1236-1248,
643 doi:<https://doi.org/10.1016/j.oregeorev.2016.06.022> (2017).

644 79 Baalousha, M. *et al.* Discovery and potential ramifications of reduced iron-bearing
645 nanoparticles—magnetite, wüstite, and zero-valent iron—in wildland–urban interface fire ashes.
646 *Environmental Science: Nano* **9**, 4136-4149, doi:10.1039/D2EN00439A (2022).

647 80 Silva, L. F. O., Schindler, M., Alavijeh, M. A., Finkelman, R. B. & Oliveira, M. L. S. A review of the
648 mineralogical and chemical composition of nanoparticles associated with coal fires. *Journal of
649 Environmental Quality* **51**, 1103-1117, doi:<https://doi.org/10.1002/jeq2.20409> (2022).

650 81 Bodí, M. B. *et al.* Wildland fire ash: Production, composition and eco-hydro-geomorphic effects
651 (vol 130, pg 103, 2014). *Earth-Science Reviews* **138**, 503-503,
652 doi:10.1016/j.earscirev.2014.07.005 (2014).

653 82 Querol, X. *et al.* Influence of soil cover on reducing the environmental impact of spontaneous
654 coal combustion in coal waste gob: A review and new experimental data. *International Journal
655 of Coal Geology* **85**, 2-22, doi:<https://doi.org/10.1016/j.coal.2010.09.002> (2011).

656 83 Stracher, G. B. & Stracher, G. B. in *Geology of Coal Fires: Case Studies from Around the World*
657 Vol. 18 0 (Geological Society of America, 2007).

658 84 Reich, M. *et al.* Formation of cristobalite nanofibers during explosive volcanic eruptions. *Geology*
659 **37**, 435-438, doi:10.1130/G25457A.1 (2009).

660 85 Larocque, A. C. L. *et al.* Deposition of a high-sulfidation Au assemblage from a magmatic volatile
661 phase, Volcán Popocatépetl, Mexico. *Journal of Volcanology and Geothermal Research* **170**, 51-
662 doi:<https://doi.org/10.1016/j.jvolgeores.2007.09.009> (2008).

663 86 Taran, Y. A., Bernard, A., Gavilanes, J.-C. & Africano, F. Native gold in mineral precipitates from
664 high-temperature volcanic gases of Colima volcano, Mexico. *Applied Geochemistry* **15**, 337-346,
665 doi:[https://doi.org/10.1016/S0883-2927\(99\)00052-9](https://doi.org/10.1016/S0883-2927(99)00052-9) (2000).

666 87 Stolzenburg, D. *et al.* Atmospheric nanoparticle growth. *Reviews of Modern Physics* (2023).

667 88 Kulmala, M. How particles nucleate and grow. *Science* **302**, 1000-1001,
668 doi:10.1126/science.1090848 (2003).

669 89 Eyring, V. *et al.* *Climate Change 2021: The Physical Science Basis. Contribution of Working
670 Group 1 to the Sixth Assessment Report of the Intergovernmental Panel on Climate Change;
671 Chapter Three; Human influence on the climate system.* (2021).

672 90 Lelieveld, J., Evans, J. S., Fnais, M., Giannadaki, D. & Pozzer, A. The contribution of outdoor air
673 pollution sources to premature mortality on a global scale. *Nature* **525**, 367-371,
674 doi:10.1038/nature15371 (2015).

675 91 Yang, Y. *et al.* Discovery and ramifications of incidental Magnéli phase generation and release
676 from industrial coal-burning. *Nature Communications* **8**, 194, doi:10.1038/s41467-017-00276-2
677 (2017).

678 92 McDaniel, D. K. *et al.* Pulmonary Exposure to Magnéli Phase Titanium Suboxides Results in
679 Significant Macrophage Abnormalities and Decreased Lung Function. *Front Immunol* **10**, 2714,
680 doi:10.3389/fimmu.2019.02714 (2019).

681 93 Guo, Y., Teixeira, J. P. & Rytí, N. Ambient Particulate Air Pollution and Daily Mortality in 652
682 Cities. *New England Journal of Medicine* **381**, doi:10.1056/NEJMoa1817364 (2019).

683 94 Alshehri, T. *et al.* Wildland-urban interface fire ashes as a major source of incidental
684 nanomaterials. *Journal of Hazardous Materials* **443**, 130311, doi:10.1016/j.jhazmat.2022.130311
685 (2022).

686 95 Aguilera, R., Corringham, T., Gershunov, A. & Benmarhnia, T. Wildfire smoke impacts respiratory
687 health more than fine particles from other sources: observational evidence from Southern
688 California. *Nature Communications* **12**, 1493, doi:10.1038/s41467-021-21708-0 (2021).

689 96 Wirth, R., Reid, D. & Schreiber, A. Nanometer-sized platinum-group minerals (PGM) in base
690 metal sulfides: New evidence for an orthomagmatic origin of the Merensky Reef PGE ore
691 deposit, Bushveld Complex, South Africa. *The Canadian Mineralogist* **51**, 143-155,
692 doi:10.3749/canmin.51.1.143 (2013).

693 97 Helmy, H. M. *et al.* Noble metal nanoclusters and nanoparticles precede mineral formation in
694 magmatic sulphide melts. *Nature Communications* **4**, 2405, doi:10.1038/ncomms3405 (2013).

695 98 Junge, M., Wirth, R., Oberthür, T., Melcher, F. & Schreiber, A. Mineralogical siting of platinum-
696 group elements in pentlandite from the Bushveld Complex, South Africa. *Mineralium Deposita*
697 **50**, 41-54 (2014).

698 99 McLeish, D. F., Williams-Jones, A. E., Vasyukova, O. V., Clark, J. R. & Board, W. S. Colloidal
699 transport and flocculation are the cause of the hyperenrichment of gold in nature. *Proceedings
700 of the National Academy of Sciences* **118**, e2100689118, doi:doi:10.1073/pnas.2100689118
701 (2021).

702 100 Duan, H., Wang, C., Hu, R., Zhu, J. & Deng, J. Supernormal enrichment of cadmium in sphalerite
703 via coupled dissolution-reprecipitation process. *Communications Earth & Environment* **4**, 356,
704 doi:10.1038/s43247-023-01025-8 (2023).

705 101 Chorover, J., Kretzschmar, R., Garcia-Pichel, F. & Sparks, D. L. Soil Biogeochemical Processes
706 within the Critical Zone. *Elements* **3**, 321-326, doi:10.2113/gselements.3.5.321 (2007).

707 102 Cron, B., Macalady, J. L. & Cosmidis, J. Organic Stabilization of Extracellular Elemental Sulfur in a
708 Sulfurovum-Rich Biofilm: A New Role for Extracellular Polymeric Substances? *Front Microbiol* **12**,
709 720101, doi:10.3389/fmicb.2021.720101 (2021).

710 103 Masuda, H., Peacor, D. R. & Dong, H. Transmission electron microscopy study of conversion of
711 smectite to illite in mudstones of the Nankai Trough: Contrast with coeval bentonites. *Clays and
712 Clay Minerals* **49**, 109-118 (2001).

713 104 Cho, H. D. & Mermut, A. R. Evidence for Halloysite Formation from Weathering of Ferruginous
714 Chlorite. *Clays and Clay Minerals* **40**, 608-619, doi:10.1346/CCMN.1992.0400516 (1992).

715 105 Schindler, M. & Hochella, M. F. Sequestration of Pb-Zn-Sb- and As-bearing incidental
716 nanoparticles by mineral surface coatings and mineralized organic matter in soils. *Environmental
717 Science: Processes & Impacts* **19**, 1016-1027, doi:10.1039/C7EM00202E (2017).

718 106 González-Jiménez, J. M. *et al.* Polymetallic nanoparticles in pyrite from massive and stockwork
719 ores of VMS deposits of the Iberian Pyrite Belt. *Ore Geology Reviews* **145**, 104875,
720 doi:<https://doi.org/10.1016/j.oregeorev.2022.104875> (2022).

721 107 Hough, R. M., Noble, R. R. P. & Reich, M. Natural gold nanoparticles. *Ore Geology Reviews* **42**,
722 55-61, doi:<https://doi.org/10.1016/j.oregeorev.2011.07.003> (2011).

723 108 Kennedy, C. B., Scott, S. D. & Ferris, F. G. Characterization of Bacteriogenic Iron Oxide Deposits
724 from Axial Volcano, Juan de Fuca Ridge, Northeast Pacific Ocean. *Geomicrobiology Journal* **20**,
725 199-214, doi:10.1080/01490450303873 (2003).

726 109 Spiro, T. G., Bargar, J. R., Sposito, G. & Tebo, B. M. Bacteriogenic manganese oxides. *Acc Chem
727 Res* **43**, 2-9, doi:10.1021/ar800232a (2010).

728 110 Gharieb, M. M., Wilkinson, S. C. & Gadd, G. M. Reduction of selenium oxyanions by unicellular,
729 polymorphic and filamentous fungi: Cellular location of reduced selenium and implications for
730 tolerance. *Journal of Industrial Microbiology* **14**, 300-311, doi:10.1007/bf01569943 (1995).

731 111 Falciatore, A. & Bowler, C. Revealing the molecular secrets of marine diatoms. *Annu Rev Plant
732 Biol* **53**, 109-130, doi:10.1146/annurev.arplant.53.091701.153921 (2002).

733 112 Rea, I., Terracciano, M. & De Stefano, L. Synthetic vs Natural: Diatoms Bioderived Porous
734 Materials for the Next Generation of Healthcare Nanodevices. *Adv Healthc Mater* **6**,
735 doi:10.1002/adhm.201601125 (2017).

736 113 Hu, S. Identification of greigite in lake sediments and its magnetic significance. *Science in China
737 Series D* **45**, 81, doi:10.1360/02yd9009 (2002).

738 114 Chang, L. *et al.* Identification and environmental interpretation of diagenetic and biogenic
739 greigite in sediments: A lesson from the Messinian Black Sea. *Geochemistry, Geophysics,
740 Geosystems* **15**, 3612-3627, doi:<https://doi.org/10.1002/2014GC005411> (2014).

741 115 Moreau, J. W., Webb, R. I. & Banfield, J. F. Ultrastructure, aggregation-state, and crystal growth
742 of biogenic nanocrystalline sphalerite and wurtzite. *American Mineralogist* **89**, 950-960,
743 doi:10.2138/am-2004-0704 (2004).

744 116 Madden, A. S. *et al.* Long-term solid-phase fate of co-precipitated U(VI)-Fe(III) following
745 biological iron reduction by Thermoanaerobacter. *97*, 1641-1652,
746 doi:doi:10.2138/am.2012.4122 (2012).

747 117 Suzuki, Y., Kelly, S. D., Kemner, K. M. & Banfield, J. F. Nanometre-size products of uranium
748 bioreduction. *Nature* **419**, 134-134, doi:10.1038/419134a (2002).

749 118 Vetriani, C. *et al.* Mercury adaptation among bacteria from a deep-sea hydrothermal vent. *Appl
750 Environ Microbiol* **71**, 220-226, doi:10.1128/aem.71.1.220-226.2005 (2005).

751 119 Meeker, K. A., Chuan, R. L., Kyle, P. R. & Palais, J. M. Emission of elemental gold particles from
752 Mount Erebus, Ross Island, Antarctica. *Geophysical Research Letters* **18**, 1405-1408,
753 doi:<https://doi.org/10.1029/91GL01928> (1991).

754 120 Stolzenburg, D. *et al.* Atmospheric nanoparticle growth. *Reviews of Modern Physics* **95**, 045002,
755 doi:10.1103/RevModPhys.95.045002 (2023).

756 121 Baurier Aymat, S. *et al.* Nanoscale Structure of Zoned Laurites from the Ojén Ultramafic Massif,
757 Southern Spain. *Minerals* **9**, 288, doi:10.3390/min9050288 (2019).

758 122 Jiménez-Franco, A. *et al.* Nanoscale constraints on the in situ transformation of Ru–Os–Ir
759 sulfides to alloys at low temperature. *Ore Geology Reviews* **124**, 103640,
760 doi:<https://doi.org/10.1016/j.oregeorev.2020.103640> (2020).

761 123 Xiong, F. *et al.* Mineralogical and isotopic peculiarities of high-Cr chromitites: Implications for a
762 mantle convection genesis of the Bulqiza ophiolite. *Lithos* **398-399**, 106305,
763 doi:<https://doi.org/10.1016/j.lithos.2021.106305> (2021).

764

765

Fig. 1. Schematic overview of various pathways of nanomaterial formation in aqueous fluids within the critical zone (the sketch of the critical zone is adapted from ¹⁰¹). Note that the upper half of the schematic is for biotic-controlled pathways, and the lower half for abiotic-controlled pathways.

766

Fig. 2 Abiotic pathways of nanomaterial formation. (a)-(b) Example for pathway *la2*: Scanning-TEM (STEM) images of the formation of gold nanoparticles (Au NP's) along the interface of pyrite and Fe-oxides (Fe-Ox); (c)-(d) Example for pathway *la3* (and for *la1* if the Ag₂S grains are considered to be nano in size): (c) STEM image and (d) STEM-EDS chemical distribution map for Ag (red) and Hg (green) indicating the replacement of a Ag₂S grain (on the right) by HgS (green rim) ³² , (e)-(f) Example for pathway *la4*: TEM images of the simultaneous formation of ferrihydrite and amorphous silica NM during the weathering of volcanic glass ³³; (e) overview image depicting areas with high ("Fe-rich area") and low ("glass") degree of weathering; (f) higher magnification image of individual ferrihydrite particles (in the lower nanometer-size range) embedded in an amorphous silica matrix; (g)-(h) Example for pathway *Ib1*: SEM-BSE image of a part of a mineral surface coating on a Fe-rich pyroxene and TEM image depicting numerous Fe-(hydr)oxide formed in the matrix of an amorphous Fe-silica phase ³⁵ , the area depicted in (h) is indicated with a white square in (g); (a), (b) (g) and (h) are unpublished images from features previously shown in 20,35; (c)-(f) are published with permission.

767

768

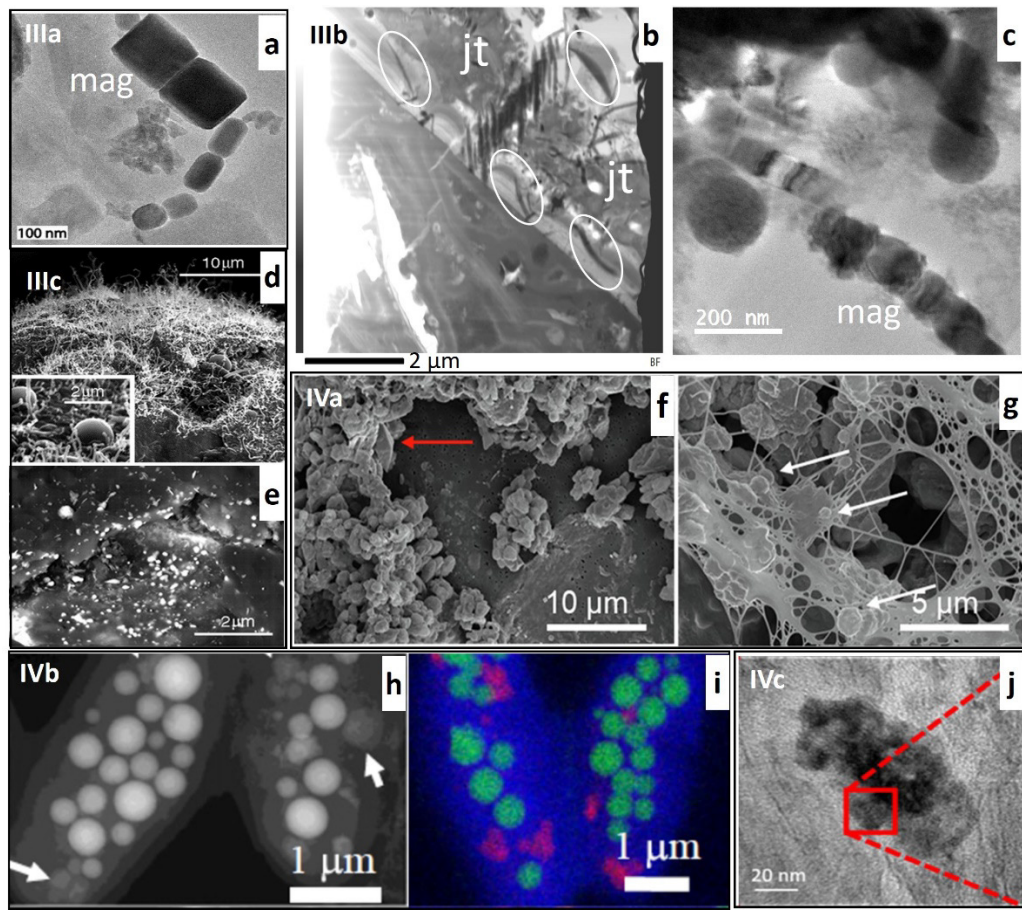


Fig 3 Biotic pathways of nanomaterial formation. (a) Example for pathway IIIa: transmission electron micrographs (TEM) of magnetite NMs (mag) formed via microbial alteration of hematite⁶³; (b)-(c) example for IIIb: (b) scanning TEM image of a focused ion beam section extracted from a soil sample obtained near a smelting center in Ontario, Canada; occurrences of petrified spirilla with the same orientation on the surface of jarosite (jt) are encircled; (c) TEM image of biogenic magnetite NMs (mag) in close proximity to one of the spirilla encircled in (b)³⁵; (d)-(e) example for IIIC: scanning electron micrographs (SEM) of gold NMs in biofilms through biological alteration of gold-containing ores⁶⁹; (f)-(g) example for IVa: SEM of elemental sulfur formed in Sulfurovum-dominated streamer biofilms in the Frasassi Cave, Italy¹⁰²; (h)-(i) example for IVb: TEM and STEM-EDS analysis of calcium carbonate nanoparticles (green) and polyP granules (red) formed inside cyanobacteria⁶⁸; (j) example for IVc: TEM of metacinnabar nanoparticles formed in sulfidic niches of contaminated streambank soil⁷⁴; Figures (a) and (d)-(j) are with permission and (b)-(c) are unpublished images from features shown in³⁵.

Table 1. Formation mechanisms of natural and incidental NMs in fluids**I. Abiotic formation coupled in space and time with weathering and alteration**

Location or environment of weathering/alteration	Parent	Daughter NM	Reference
a. Formation of a first-generation NMs			
1. Formation of NM replacing a first generation of NM			
Oceanic bentonite-sediments in subduction zone; altered rhyolitic hyaloclastite	Smectite	Interstratified illite-smectite mixtures with various illite-smectite ratios	14,103
Soils, sediments	Ferrihydrite	Nano-Goethite or hematite	33
Soils, sediments and wastewater	Engineered or incidental Ag nanoparticles	Ag ₂ S NM	16
2. Formation of only one type of NM which contains a minor element of the parent			
Alteration of ultra-basic rocks during greenschist metamorphisms	Cr-rich pyroxenes	Clinochlore (bulk) + chromite NMs	21
Low-T alteration	Au-bearing pyrite	Au NM + hematite (bulk)	20. Fig. 2a, b
Hydrothermal alteration	Au-bearing As-rich pyrite	Au NM + polycrystalline matrix of pyrite and arsenopyrite	19
3. Formation of only one type of NM which contains the major element of the parent			
Soil	K-Feldspar	“paracrystalline” phase or “gel”	23
Soil, sediment	Pyrite, Fe ₂ S	Ferrihydrite	24
Contaminated soils	Ag ₂ S	HgS	32, Fig. 2c, d
4. Syn-formation of more than one type of NM			
Pedogenic altered basaltic glass in	Volcanic glass	amorphous Si-Al-Fe-phase + ferrihydrite	33, Fig. 2e, f

volcanic ash (dry-cool conditions)			
Soil	Fe-rich chlorite	halloysite-kaolinite, goethite, hematite, interstratified chlorite-1:1 sheet silicate	104
b. Formation of a second or consecutive generation of NMs after the weathering/alteration of a first-generation nano-daughter phase			
1. Formation of NM via amorphous precursors			
Location or environment of weathering/alteration	Parent	Daughter NM	Reference
Soil	K-Feldspar	“protocrystalline layer” depleted in Ca, Na, K and Si, enriched in Fe → halloysite and kaolinite	34
Soil	Fe-rich pyroxene	1 st Generation: amorphous Fe-Si-rich matrix → green rust 2 nd generation: goethite, magnetite, jarosite, Ni-rich spinel; 3 rd generation: P-rich ferrihydrite → illite+chlorite	35, Fig. 2g, f
2. Formation of chemically related NMs with the addition or removal of minor constituents from the alteration layer			
Soil, Weathering profiles	Biotite	oxybiotite → vermiculite → kaolinite + Fe/Al oxyhydroxides	36,37
Soil	Muscovite	Illite-smectite → smectite → kaolinite	34
3. Formation of chemically related NMs with the addition or removal of a major constituent from the alteration layer			
Mine tailings	Pyrite	Weak acidic to basic pH range: ferrihydrite → goethite	24,38
Groundwater	Uraninite	Si-rich uraninite → coffinite	39,40
II. Abiotic formation decoupled in space and time with weathering and alteration			

a. Heterogeneous nucleation of NMs on chemically reactive redox sites in pores or on surfaces			
Environment	Host	NM	Reference
Soils	Organic matter	Cu or Ag through reduction of Cu ^{+/2+} and Ag ⁺ on functional groups	41-43, 17
Hydrothermal	Fe-bearing phyllosilicates	Cu in interlayer, reduction by Fe ²⁺	44-48
b. Heterogeneous nucleation of NMs on sites in pores or on surfaces			
Soils	Pores in organic matter	amorphous silica → Cu-Zn-bearing magnetite (Fe ₃ O ₄), cuprite (Cu ₂ O) and spertiniite (Cu(OH) ₂)	51
Soils	Pores in mineralized organic matter	franklinite	105
Soils	Fungi	Ca-oxalate	52
Soils	Interior surface of plant	Au	55
Soils and tailings	Bacteria	clays and silica	53
Tailings	Granite	Schwertmannite	54
Various types of hydrothermal ore deposits	Pyrite, As-rich pyrite Arsenopyrite	Au, other types of sulfides, sulfarsenides	19,106,107
c. Homogeneous nucleation of NMs due to changes in pH, P, T, O ₂ fugacity and activity of species			
Environment	Variables/Processes	NM	Reference
1. Low T processes			
Riverine system	pH from acidic organic rich to neutral with less organics	Ferrihydrite	58
Riparian Zone	Changes in redox conditions	Ferrihydrite	59
2. High T processes			

Black smokers	P, T and mixing with seawater	Au, Bi, sulfides tellurides	61
Black smokers	P around ascending fluids	Au	60
Epithermal ore deposits	coagulation of Au NM due to cooling/boiling/catalysis	Au	62
III. Biotic formation coupled in space and time with weathering and alteration			
a. Formation of NMs through energy metabolisms (redox reactions) of organisms			
Environment	Parent	Daughter NM	Reference
Mineral surface coatings in soils and Quaternary sediments	hematite/jarosite	Magnetite	63, Fig 3a
b. Formation of NMs that directly provide beneficial functions for the organism			
Environment	Parent	NM	Reference
Mineral surface coatings in soils	Jarosite	Magnetite	35, Fig. 3b-c
c. Formation of NMs involving organismal cellular components or through reactions with metabolites			
Mechanism	Parent	NM	Reference
biological mobilization and concentration of platinum-group elements within biofilms	ore grains	platinum-palladium	70
biological mobilization and concentration of gold within biofilms	gold-containing grains	Au	69, Fig. 3d-e
d. Formation of NMs within extracellular polymeric matrices			
Mechanism	Parent	NM	Reference
photochemistry-driven transformation	extracellular polymeric substances (freshwater lakes)	protein-like transparent particles	71

IV. Biotic formation decoupled in space and time with weathering and alteration			
a. Formation of NMs through energy metabolisms (redox reactions) of the organism			
Mechanism	Parent	NM	Reference
bacterial sulfur oxidation	hydrogen sulfide (from microbial sulfate reduction or hydrothermal venting)	elemental sulfur	67
Bacterial oxidation of sulfide for energy	Hydrogen sulfide	elemental sulfur	102, Fig. 3f-g
bacterial iron oxidation for energy	dissolved Fe(II)	2-line ferrihydrite, goethite, and amorphous phases	108
bacterial manganese oxidation for energy	dissolved Mn(II)	manganese (IV)/(III) oxide	109
fungal reduction of selenite	Dissolved Se	Selenium	110
b. Formation of NMs that directly provide beneficial functions for the organism			
Environment	Location	NM	Reference
A range of environments where cyanobacteria thrive	intracellular biomineralization (regulating bacterial buoyancy)	calcium carbonate	68, Fig. 3h-i
Marine and freshwater	intracellular biomineralization (storing iron source)	hydrated amorphous silica	111,112
c. Formation of NMs involving organismal cellular components or through reactions with metabolites			
Environment	Parent	NM	Reference
a range of anoxic/sulfide-rich environments	Microbial-reduced sulfate species	iron sulfide (greigite, mackinawite, pyrite, and pyrrhotite)	66
Lake sediments	sedimentary sulfate	Greigite	113
Messinian Black Sea sediments	Terrigenous input of sulfate	Greigite	114

Abandoned mine	microbial reduced sulfate	Sphalerite	115
contaminated streambank soils	biological- sulfidation	Metacinnabar	74, Fig. 3j
groundwater aquifers, uranium deposits/tailings	microbially mediated reduced species (usually through iron reduction or sulfate-reduction)	Uraninite	116,117
deep sea hydrothermal vents	biologically mediated reduction/adaptation of Hg species	Mercury	118

770

771

772

773

774

775

776

777

778

779

780

781

782

783

784

785

786

787

788

789

790

791 **Table 2. Formation mechanisms of natural and incidental NMs in the gas phase and**
 792 **during magmatic processes**

793

V. Abiotic pathways of NM formation in the gas phase: thermal decomposition, volatilization, oxidation, sublimation, solidification, freezing and thermal alteration during incidental combustions			
a. High-T processes			
Environment	Variables/Processes	NM	Reference
1. Wild- and coal fires			
Soil-plant interface	Wildfires set by lightning	amorphous carbon CaCO ₃ , FeCl ₂ , FeSO ₄ Fe(NO ₃) ₃ , FeCl ₃ , magnetite	79,94
Thermal alteration aureoles along coal-sediment interface	Coal fires set through spontaneous combustion or lightning	soot, nanotubes, fullerenes, tar at high T: oxides and silicates at < 630°C: sulfates and sulfides	80
2. Volcanic activities			
Volcanic fumaroles	Changes in T	Au	85,86,119
Volcanic eruptions	Redox reactions between silica glass and carbon monoxide	Cristobalite	84
b. Low T processes			
Environment	Process/source	NM	Reference
1. Freezing			
Troposphere to Stratosphere	Freezing	ice, crystalline acid hydrates such as H ₂ SO ₄ ·4H ₂ O, HNO ₃ · 3H ₂ O	75
2. New particle formation			
Lower troposphere	New particle formation through oxidation of S- and N- species and organic components	mascagnite, (NH ₄) ₂ SO ₄ , critical nuclei containing sulfates, nitrates, organic matter	75,76,120

	from natural (e.g. volcanic eruptions) and anthropogenic sources		
3. Sea spray			
CZ to Lower troposphere	Nucleation from sea spray, often associated with other atmospheric particles	halite, NaCl, gypsum, $\text{CaSO}_4 \cdot 2\text{H}_2\text{O}$, glauberite, $\text{Na}_2\text{Ca}(\text{SO}_4)_2$, loweite, $\text{Na}_{12}\text{Mg}_7(\text{SO}_4)_{13}$	77
VI. Pathways of NM formation during magmatic processes			
Host/environment	Processes	NM	References
pyrrhotite, millerite, pyrite, pentlandite and chalcopyrite in mafic-ultramafic Rocks	Changes in T, fO_2 and activity of sulfide and silica	PGE-alloys, -sulfides, -tellurides, -stannides	96,98,121-123

794

795

796

797